JOURNAL OF MATERIALS SCIENCE 25 (1990) 1917–1923

Mechanical behaviour of poly(methyl methacrylate)

Part 1 Tensile strength and fracture toughness

W.-M. CHENG*¶, G. A. MILLER‡, J. A. MANSON*†‡, R. W. HERTZBERG‡, L. H. SPERLING§‡
*Department of Chemistry, ‡Department of Materials Science and Engineering and §Department of Chemical Engineering, Center for Polymer Science and Engineering, Materials Research Center, Whitaker Laboratory 5, Lehigh University, Bethlehem, Pennsylvania 18015, USA

A series of tensile and three-point bending studies was conducted at various temperatures and loading rates using a commercial poly(methyl methacrylate) (PMMA). Tensile properties and fracture toughness data were obtained for the various conditions. In general, both tensile strength and fracture toughness increase with increasing loading rate and decreasing temperature. However, when the temperature reaches the glass transition region, the relationships between fracture toughness, loading rate, and temperature become very complex. This behaviour is due to the simultaneous interaction of viscoelasticity and localized plastic deformation. In the glass transition region, the fracture mechanism changes from a brittle to a ductile mode of failure. A failure envelope constructed from tensile tests suggests that the maximum elongation that the glassy PMMA can withstand without failure is about 130%. The calculated apparent activation energies suggest that the failure process of thermoplastic polymers (at least PMMA) follows a viscoelastic process, either glass or β transition. The former is the case if crack initiation is required.

1. Introduction

Considerable effort has been devoted to the determination of the tensile strength and fracture toughness of many polymers. In particular, poly(methyl methacrylate) (PMMA) is one of the most intensively studied polymers [1–5]. PMMA is an amorphous glass below about 110° C and exhibits brittle fracture under normal conditions below about 80° C. This material also possesses consistent properties for a given set of experimental conditions. Also, it has long been realized by engineers that some materials which exhibit great strength or toughness under low-strain rate or at high temperature will fracture easily when hit with a sharp blow. Polymeric materials, because of their viscoelasticity, are extremely sensitive to strain rate and temperature. It is a well known observation that as the temperature decreases, or loading rate increases, both yield stress (σ_{ys}) and Young's modulus (E) increase.

Much of the variation in the published data on fracture toughness of PMMA can be explained when the data are correlated as a function of loading rate. However, for temperatures other than room temperature, the data are less plentiful and there is considerable variation between the results quoted by various authors [6]. The purpose of the present work is to study the effects of temperature and loading rate on the tensile strength (σ_{UTS}) and fracture toughness (K_C) of PMMA. If quantitative relationships between σ_{UTS}, K_C, and both temperature and loading rate can be developed, they will be of use in formulating and evaluating models for fatigue crack propagation in PMMA.

2. Experimental details

2.1. Tensile strength

Commercial poly(methyl methacrylate) (PMMA) supplied by Rohm and Haas (M_n = 478 000 g mol^{-1}) was used in this work. Tensile specimens (ASTM D638 Type I) [7] were machine-cut from the cast PMMA sheet of 1/4 inch (6.35 mm) thickness. After machining, the specimen was inserted in grips, and uniaxial stress–strain relations were determined using an Instron Universal tensile testing machine. The load and crosshead displacement were recorded on a strip chart recorder.

The details of the testing procedures used are described in ASTM D638. The experiments were conducted as a function of strain rate and temperature. The strain rate ranged over three decades from 0.017 to 0.00017 sec^{-1} (corresponding to crosshead speeds from 2 to 0.002 in min^{-1}), and temperatures varied from room temperature to 100° C. Strains and strain rates were calculated from the specimen gauge length and crosshead displacement which were measured as a function of time. The temperature was controlled by a thermal tape which was wrapped around the reduced section of the specimen. Temperature was measured with a thermocouple mounted at the centre of the specimen gauge length. Several tensile properties, such

† Deceased.
¶ *Present address*: Borden Chemicals and Plastics, R & D Laboratory, P.O. Box 427, Geismar, LA 70734, USA.

0022–2461/90 $03.00 + .12

as tensile strength, per cent elongation, modulus of elasticity, yield stress, were calculated based on the load–displacement curves.

2.2. Fracture toughness

2.2.1. Specimen

Specimens of the same cast PMMA sheet were machined into the three-point-bend (also called single edge notched bend, SENB) geometry, defined by ASTM E399 [8]. The initial saw-cut notch had a length in the range of $0.45 < a/W < 0.55$, where a and W are notch length and specimen width, respectively. The notched specimen was then precracked by either pressing in or sliding a sharp razor blade into the notch root. Initial crack lengths were measured with an optical microscope.

2.2.2. Experimental conditions

The three-point bending procedures were based on ASTM E399 and D790 [8, 9]. In order to investigate the dependence of fracture toughness on temperature and loading rate, studies were conducted at loading rates from 0.2 to 22 000 N sec^{-1}, and over a temperature range from -30 to 100° C which includes T_β and approaches the glass transition temperature of PMMA.

The measurements were made in an Instron testing machine fitted with an oven for controlling temperature. The accuracy of temperature control was about ± 1° C and was monitored by using a feedback control system and a thermocouple. Measurements were performed under constant loading rate control. The load–crosshead displacement curves were recorded by both an X–Y–Y recorder and a storage oscilloscope. At least three replicates were tested for each condition.

2.2.3. Calculations

Several important material properties, such as fracture toughness (K_C), fracture energy release rate (G), Young's modulus (E), can be calculated from the load–displacement curve of the three-point bending experiments.

2.2.3.1. Fracture toughness

Values of fracture toughness (K_C) can be computed from the original crack length according to the following relationships for an SENB specimen [8, 10].

$$K_C = \left(\frac{P_Q S}{BW^{3/2}}\right) Y(a/W) \quad (1)$$

$$Y(a/W) = \frac{3(a/W)^{1/2}\left[1.9 - \left(\frac{a}{W}\right)\left(1 - \frac{a}{W}\right)\left(2.15 - 3.93\frac{a}{W} + 2.7\frac{a^2}{W^2}\right)\right]}{2\left(1 + 2\frac{a}{W}\right)\left(1 - \frac{a}{W}\right)^{3/2}} \quad (2)$$

where S = span length, 2 inches in this work;
P_Q = maximum load on the load-deflection curve;
B = specimen thickness;
W = specimen width;
a = initial crack length.

If K_C satisfies the conditions that both B and a are greater than $2.5(K_{IC}/\sigma_{ys})^2$, then K_C is equal to K_{IC}, the plane strain fracture toughness.

The determination of P_Q is described in ASTM E399. Under certain conditions encountered in this study, specimens failed in a ductile fashion; i.e. the experimental conditions did not match the requirements of ASTM E399. In those cases, the toughness value was computed for P_Q.

2.2.3.2. Energy release rate

The energy release rate (G) can, in principle, be obtained from the relationship of $EG = K_C^2$. However, many uncertainties are introduced by this procedure and thus, it is considered preferable to determine G directly from the energy (U) derived from integrating the area under the load against load-point deflection diagram up to the same load as used for determination of K_C [11]. In this case, G may be calculated according to Equation 3.

$$G = U/BW\phi \quad (3)$$

The energy calibration factor ϕ may be computed from $Y(a/W)$ and the compliance [12].

2.2.3.3. Young's modulus

There are two ways to calculate Young's modulus (E). The first method is based on the initial loading compliance [11]. The measured initial slope of load-deflection diagram can be converted into initial compliance. The second method to compute Young's modulus is based on the relationships of $K_C^2 = EG$ for the plane stress condition, and $K_{IC}^2 = EG/(1 - \nu^2)$ for the plane strain condition [10], where ν is Poisson's ratio. After calculating G from the deformation energy, E may thus be obtained based on these two relationships, according to the experimental conditions.

2.2.3.4. Plastic zone size

The elastic analysis predicts infinite stress at the crack tip, but local yielding prevents this from happening. The region around the crack tip in which the effective stress is equal to the yield stress is called the plastic zone. Irwin [13] related to the plastic zone size to the magnitude of the applied stress intensity level and material yield strength, and estimated it to be,

$$r_y = \frac{\pi}{2}(K/\sigma_{ys})^2 \text{ (plane stress)} \quad (4)$$

$$r_y = \frac{\pi}{6}(K/\sigma_{ys})^2 \text{ (plane strain)} \quad (5)$$

where r_y = plastic zone radius;
K = stress intensity factor;
σ_{ys} = yield strength.

3. Results

3.1. Stress–strain analysis

The current results show that the per cent elongation increases with increasing temperature and decreasing

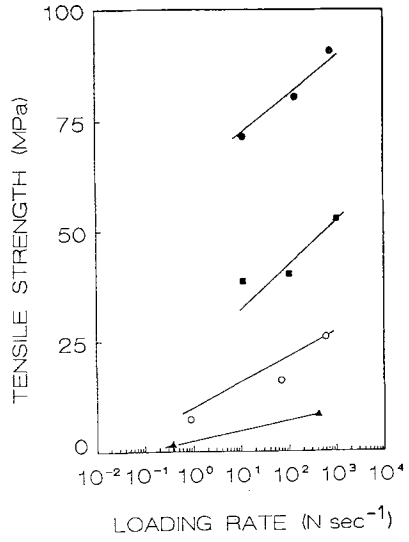

Figure 1 The relationships between tensile strength and loading rate at different experimental temperatures of poly(methyl methacrylate). The straight lines represent Equation 6. (●) 24° C; (■) 60° C; (○) 80° C; (▲) 100° C.

loading rate. Young's modulus and tensile strength, on the other hand, increase with decreasing temperature and increasing loading rate. These trends are depicted in Table I and Figs 1 and 2. The strain rate sensitivity, increase in strength for a given change in loading rate, is highest at room temperature and lowest at 100° C (see Fig. 1).

By performing a linear regression analysis, the relationship between strength, temperature, and loading rate was found to be described by Equation 6.

$$\sigma_{UTS} = -2.94 \times 10^{8} + \frac{1.09 \times 10^{11}}{T} + 2.3 \times 10^{6} \log (R) + 4.47 \times 10^{6} \left(\frac{R}{T}\right) \quad (6)$$

where, σ_{UTS} = tensile strength, Pa;
T = temperature, °K:
R = loading rate, N sec^{-1}.

The correlation coefficient for this regression was 0.98.

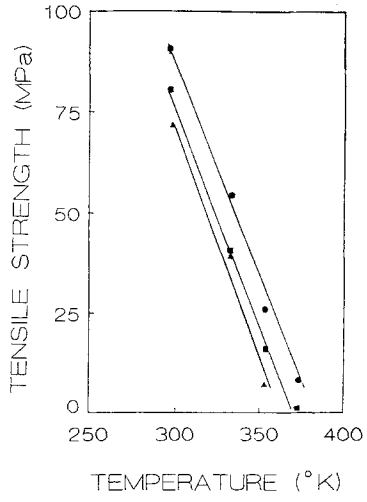

Figure 2 The relationships between tensile strength and experimental temperature at different crosshead rates. The straight lines represent Equation 6. (●) 2 inch min^{-1}; (■) 0.2 inch min^{-1}; (▲) 0.02 inch min^{-1}.

3.2. Fracture toughness

A criterion for the plane strain condition has been described in ASTM E399. In order to meet such conditions, both the specimen thickness, B, and the crack length, a, must exceed 2.5 $(K_{IC}/\sigma_{ys})^2$. σ_{ys} is the yield stress, and K_{IC} is the plane strain fracture toughness for the given temperature and loading rate. The specimen thickness and the initial crack length in this work are both about 1/4 inch (6.35 mm); thus, as long as the 2.5 $(K_{IC}/\sigma_{ys})^2$ < 6.35 mm, the particular experiment will meet the plane strain criterion.

In general, studies at temperatures below 80° C and/or loading rates above 220 N sec^{-1} satisfy plane strain conditions and K_{IC} increases with increasing loading rate and decreasing temperature, Fig. 3. Those experiments at higher temperature (e.g. 100° C) and lower loading rate (e.g. < 220 N sec^{-1} at 80° C, or < 2200 N sec^{-1} at 100° C) represent the plane stress condition with the plane stress fracture toughness, K_C, decreasing as the temperature increases or loading rate decreases. Therefore, conditions of about 80° C and 220 N sec^{-1} result in a K_C minimum with K_C increasing either at lower temperature and higher loading rate or at higher temperature and lower loading rate (see Fig. 3).

To explore the relationships among fracture toughness, temperature and loading rate, it is necessary to create an empirical equation relating these variables. In order to do this, the fracture toughness data were divided into two sets according to whether or not the plane strain criterion was satisfied.

For data within the plane strain regime, fracture toughness values show a linear relationship to both $1/T$ and log (rate) (see also Fig. 3). By multiple regression, an empirical model, Equation 7, can be developed (correlation coefficient = 0.91).

$$K_{IC} = -1.77 + \frac{980.5}{T} + 13.89 \ln \left(\frac{R}{T}\right) \quad (7)$$

where K_{IC} is the plane strain fracture toughness with units of MPa $m^{1/2}$, T is the temperature in °K, and R is the loading rate in N sec^{-1}.

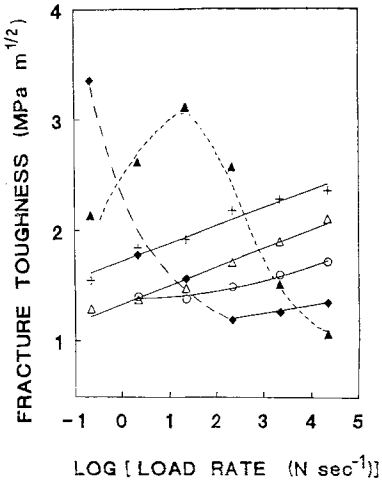

Figure 3 The relationship between three-point bending fracture toughness of poly(methyl methacrylate) and loading rate at different experimental temperatures. For the range of temperature and loading rate, the coefficient of variation for fracture toughness (standard deviation/average) ranged from 0.006 to 0.05. (▲) 100° C; (◆) 80° C; (○) 60° C; (△) 24° C; (+) 0° C.

TABLE I Average tensile properties of PMMA

Sample ID	Sample										
	2-RT	0.2-RT	0.02-RT	2-60C	0.2-60C	0.02-60C	2-80C	0.2-80C	0.02-80C	2-100C	0.2-100C
Crosshead rate (inch min^{-1})	2	0.2	0.02	2	0.2	0.02	2	0.2	0.02	2	0.2
Temperature (° C)	24.0	24.0	24.0	60.0	60.0	60.0	80.0	80.0	80.0	100.0	100.0
Gauge length (inch)	2.0	2.0	2.0	2.0	2.0	2.0	2.0	2.0	2.0	2.0	2.0
Tensile strength (MPa)	90.7	80.5	71.5	54.5	40.3	39.3	25.9	16.1	7.2	8.0	1.3
% Elongation at break	19.0	14.6	17.7	14.1	31.0	31.1	60.6	66.9	86.1	96.0	126.6
Young's modulus (MPa)	1600.0	1100.0	860.0	810.0	760.0	750.0	440.0	510.0	6.2	320.0	2.7
Initial load rate (N sec^{-1})	777.5	138.9	11.8	1027.7	103.6	10.2	598.6	67.7	0.1	436.1	0.4
Strain rate (% sec^{-1})	1.67×10^{-2}	1.67×10^{-3}	1.67×10^{-4}	1.67×10^{-2}	1.67×10^{-3}	1.67×10^{-4}	1.67×10^{-2}	1.67×10^{-3}	1.67×10^{-4}	1.67×10^{-2}	1.67×10^{-3}

Considering data outside the plane strain regime, it is found that Equation 8 fits the data at 100° C reasonably well (correlation coefficient = 0.85).

$$K_C = -9.16 - 0.32 (\ln R) + 0.000096T^2 - \frac{0.85}{(\ln R)^2} \quad (8)$$

where K_C represents the plane stress fracture toughness.

4. Discussion

Fracture toughness results depicted in Figs 3, 4, and 5 illustrate two major findings. First, for temperatures below 80° C and loading rates around 1000 N sec^{-1}, plane strain fracture toughness values increase with decreasing temperature and increasing loading rate. This increase in K_{IC} reflects the fact that the strength of PMMA is elevated by decreasing temperature (or increasing loading rate) whereas there is relatively little effect on the ductility (see Table I for data of elongation at break at 24 and 60° C and a crosshead speed of 2 inch min^{-1}). For temperatures of 80 and 100° C, plane strain conditions are mostly not satisfied, and below a given loading rate, fracture toughness values increase as loading rate decreases. This behaviour reflects the loss of constraint associated with the transition from plane strain to plane stress. At 100° C, the decrease in K_C for loading rates below about 10 N sec^{-1} most probably reflects the viscoelastic behaviour of PMMA above T_g, where it becomes too soft and loses its strength.

Plotting fracture toughness with respect to temperature. Mizutani [14] showed that in the glass transition region, fracture toughness increases with temperature up to near T_g, peaked at T_g, and then dropped off with further increasing temperature. Compared with data on Mizutani (at crosshead speed of 0.5 mm min^{-1}) [14], the present K_C data for a loading rate of 2.2 N sec^{-1} (corresponding to crosshead rate of about 0.2 mm min^{-1}), while higher at all temperatures, also show a minimum and an increase in K_C as T_g is approached, Fig. 4. Several facts might be responsible for the difference in toughness between current results

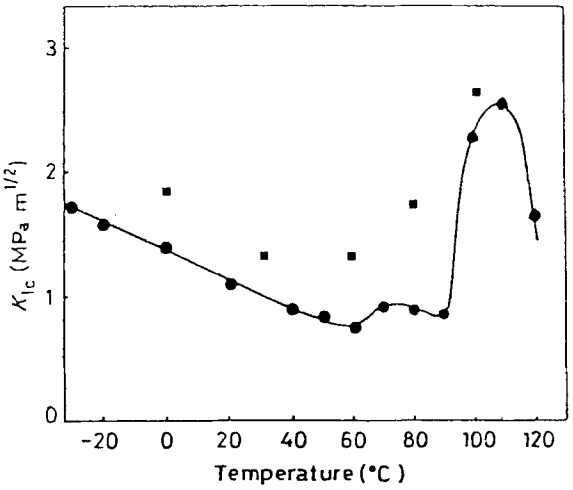

Figure 4 Fracture toughness as a function of temperature. (From [14]), solid squares represent current data at loading rate 2.2 N sec^{-1}.

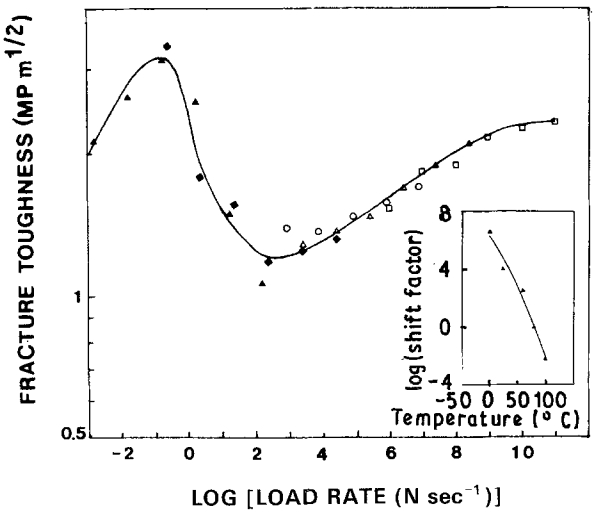

Figure 5 Master curve of relationship between fracture toughness and log (loading rate) based on Fig. 3. The reference temperature is 80° C. A glass transition peak is shown at loading rate of about 0.32 N sec^{-1}. (▲) 100° C; (◆) 80° C; (○) 60° C; (△) 24° C; (□) 0° C.

and those of Mizutani. These include possible differences in material (molecular weight, additives, etc.) and testing method (specimen geometry, control mode, etc.). At present, it is not possible to identify the source of the difference. In any case, both data sets suggest that when the temperature approaches the glass transition region, the fracture toughness increases due to enhanced plastic deformation. When the temperature exceeds T_g, the material becomes so soft and K_C decreases again. The present room temperature data measured at 220 and 22 N sec^{-1} approximately 1.65 and 1.5 MPa m$^{1/2}$ fall in the upper part of the range of published values, for PMMA, 0.8 to 1.7 MPa m$^{1/2}$ [15].

A point of practical importance is whether the time–temperature superposition principle can be applied to the fracture behaviour of PMMA in the glassy state. By arbitrarily choosing 80° C as a reference temperature, a master curve of toughness against loading rate can be constructed, Fig. 5. The procedure is to horizontally shift the curves in Fig. 3 for temperatures other than 80° C by a constant factor until they have the closest coincidence with the curve for 80° C. This procedure defines the shift factor depicted in Fig. 5. Results in Fig. 5 show that the superposition principle is valid and clearly exhibits a minimum in toughness located between T_β and T_g. The fact that the shape of the master curve in Fig. 5 is similar to that of the damping curve of the dynamic mechanical spectrum suggests that K_C should relate to energy dissipation.

Young's modulus is one of the most important material properties. As described previously, there are two ways to estimate the Young's modulus from three-point bending tests of cracked specimen. One involves using the initial loading compliance (E_i) while the second (E_c) involves separate computations of G and K and the relation $GE = K^2$. Experimental results show that E_c and E_i are proportional, Fig. 6. However, E_i values are slightly larger than E_c, and are described by the relating log E_i = 0.0344 + 1.0021 log E_c.

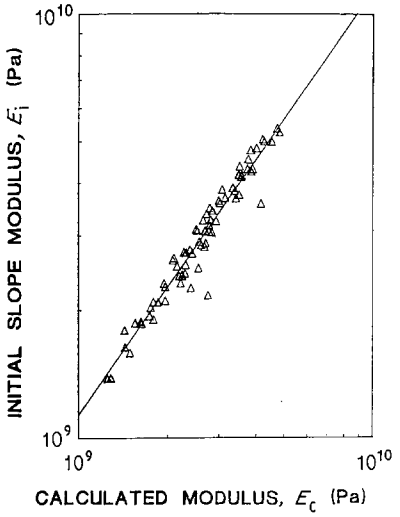

Figure 6 E_i against E_c for PMMA. E_i is the modulus based on the initial loading compliance, whereas E_c is the modulus calculated from $E_c = K^2/G$.

Figure 7 shows the relationship between E_c and temperature at different loading rates from 22000 to 0.2 N sec^{-1} (corresponding to loading frequencies from 100 to 0.001 Hz). It can be seen that the Young's modulus increases with increasing loading rate and with decreasing temperature. By choosing one Hz data (loading rate = 220 N sec^{-1}) as a reference curve, and shifting other curves at different loading rates horizontally, another master curve can be created from Fig. 7, which is shown in Fig. 8 along with the corresponding shift factors. Again, strong evidence supports the hypothesis that the time–temperature superposition principle is applicable to estimation of the modulus of PMMA in the glassy and glass transition state.

When failure points from stress–strain curves obtained at various temperatures and loading rates are plotted on one set of coordinates, the curve connecting them defines a failure envelope. The failure envelope, involving a temperature-compensated stress, serves to characterize failure properties over the

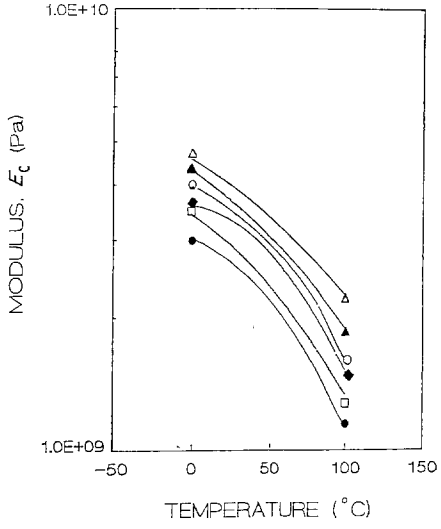

Figure 7 The relationship between PMMA modulus, E_c, calculated based on energy release rate and temperature at different loading rates. (△) 22000 N sec^{-1}; (▲) 2200 N sec^{-1}; (○) 220 N sec^{-1}; (◆) 22 N sec^{-1}; (□) 2.2 N sec^{-1}; (●) 0.2 N sec^{-1}.

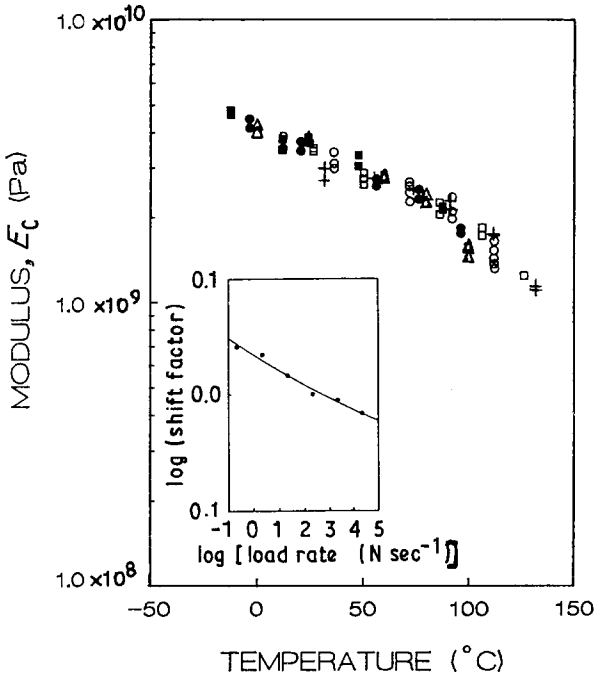

Figure 8 Master curve of the relationship between modulus and temperature based on Fig. 7. The reference loading rate is 220 N sec^{-1}.

range of temperatures and loading rates to which superposition is applicable. Although it is usually used to evaluate the properties of elastomers, it is also useful in determining the maximum strain a glassy polymer might achieve. By plotting the strain at break (ε) against the reduced breaking stress ($\sigma\ T_g/T$), a failure envelope can be constructed, Fig. 9. The failure envelope shows that the maximum elongation the PMMA can withstand without failure is about 130%.

It is of interest to determine if an Arrhenius type relationship exists between the loading rate and the reciprocal of experimental temperatures for tensile and fracture toughness data, and what the activation energies for these failure processes might be. For a constant tensile strength, the slope of the log (loading rate) against $1/T$ plot, Fig. 10, suggests that an apparent activation energy of about 270 kJ mol^{-1} for the ultimate tensile strength which is fairly close to the reported activation energy of the PMMA glass

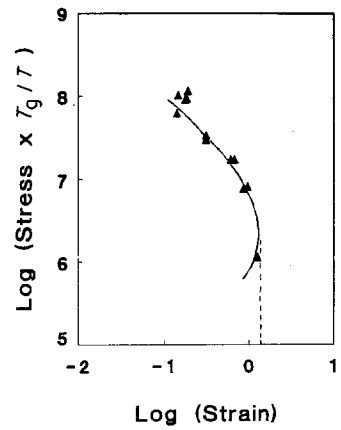

Figure 9 The tensile failure envelope of PMMA. The failure envelope shows that the maximum % elongation for amorphous PMMA is about 130.

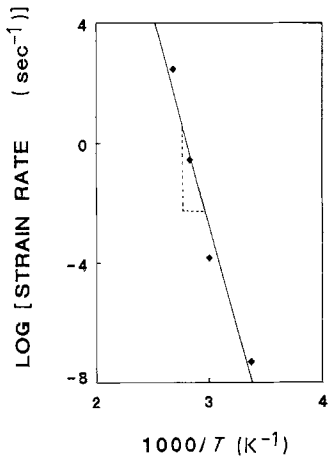

Figure 10 Arrhenius plot of PMMA based on tensile experiments. The apparent activation energy calculated from the slope is about 270 kJ mol^{-1}.

transition process (320 kJ mol^{-1}) [17]. This suggests that the failure processes in the tensile test (no pre-existing crack) may bear some relation to the microscopic processes responsible for the glass transition. On the other hand, the apparent activation energy calculated from the slope of log (loading rate) against $1/T$ plot for fracture toughness data, Fig. 11 has a value of about 120 kJ mol^{-1}, which falls into the published activation energy range for the β transition, 71–126 kJ mol^{-1} [17]. This suggests that β transition governs the fracture process in the presence of a crack [18, 19]. The experimental values of activation energy from tensile and fracture toughness experiments seem physically sensible since the former involves both initiation and propagation of a crack whereas the latter only involves crack propagation.

5. Conclusions

A series of uniaxial tensile experiments and three-point bending tests have been conducted using commercial PMMA. Based on the present study of the effects of temperature and loading rate on the tensile properties and fracture toughness, the conclusions are:

1. For temperatures below the glass transition, both tensile strength and fracture toughness increase with increasing loading rate and decreasing temperature.

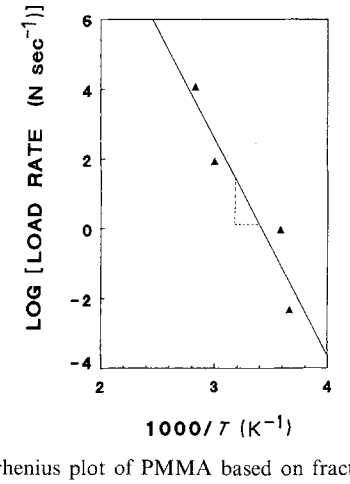

Figure 11 Arrhenius plot of PMMA based on fracture toughness experiments. The apparent activation energy calculated from the slope is about 120 kJ mol^{-1}.

2. Near the glass transition region, the fracture mechanism changes from brittle to ductile, and the relationship between fracture toughness, loading rate, and temperature becomes very complex. This is due to an interaction of the effects of localized plastic deformation and viscoelastic behaviour of the bulk material.

3. The conditions of temperature 80° C and loading rate about 220 N sec^{-1} define a saddle of minimum K_{1C}. K_{1C} increases at either lower temperature and higher loading rate or vice versa.

4. A failure envelope constructed from tensile data shows that the maximum elongation that the PMMA can withstand without failure is about 130%.

5. Arrhenius type activation energies of about 270 and 120 kJ mol^{-1} were calculated for tensile and fracture toughness processes, respectively. These apparent activation energies suggested that the failure processes of PMMA follows a viscoelastic process, either the glass or β transitions. The higher activation energy pertains to the case where crack initiation is required.

Acknowledgement

The authors wish to thank the Material Division, National Science Foundation, Grant No. DMR-8412357, Polymer Program, for financial support.

References

1. P. I. VINCENT, in "Encyclopedia of Polymer Science and Technology", Vol. 7 (John Wiley, New York, 1967) p. 292.
2. J. G. WILLIAMS, "Fracture Mechanics of Polymers", Chap 6 (John Wiley, New York, 1984).
3. H. H. KAUSCH and J. G. WILLIAMS, in "Encyclo pedia of Polymer Science and Engineering", Vol. 6, 2nd Edn. (John Wiley, New York, 1986).
4. R. SELDON, *Polym. Testing* **7** (1987) 209.
5. L. H. LEE, J. F. MANDELL and F. J. McGARRY, *Polym. Eng. Sci.* **27(15)** (1987) 1128.
6. G. P. MARSHALL, L. H. COUTTS and J. G. WILLIAMS, *J. Mater. Sci.* **9** (1974) 1409
7. Tensile properties of Plastics", ASTM D638-81, 1981.
8. Plane-Strain Fracture Toughness of Metallic Materials, ASTM E399-81, 1981.
9. Flexural Properties of Unreinforced and Reinforced Plastics and Electric Insulating Materials, ASTM D790-81, 1981.
10. R. W. HERTZBERG, "Deformation and Fracture Mechanics of Engineering Materials", 2nd edn, Chapter 8, (John Wiley, New York, 1983).
11. J. G. WILLIAMS, "A Linear Elastic Fracture Mechanics (LEFM) Standard for Determinating Kc and Gc for Plastics", ASTM D20 meeting, Palm Beach, Florida, 1987.
12. J. G. WILLIAMS, "Fracture Mechanics of Polymers", Chap 2 (John Wiley, New York, 1984).
13. G. R. IRWIN, "Handbuch der Physik", Vol. VI (Springer, Berlin, 1958) p. 49.
14. K. MIZUTANI, *J. Mater. Sci. Lett.* **6** (1987) 915.
15. G. P. MARSHALL and J. G. WILLIAMS, *ibid.* **8** (1973) 138.
16. R. W. HERTZBERG and J. A. MANSON, "Fatigue of Engineering Plastics," Chapter 3 (Academic Press, New York, 1980).
17. N. G. McCRUM, B. E. READ and G. WILLIAMS, "Anelastic and Dielectric Effects in Polymeric Solids" (John Wiley, New York, 1967).
18. R. F. BOYER, *Polym Eng. Sci.* **8(3)** (1968) 161.
19. G. P. MARSHALL, L. H. COUTTS and J. G. WILLIAMS, *J. Mater. Sci.* **9** (1974) 1409.

Received 13 October 1988
and accepted 10 April 1989